Excessive CD11c^{+}Tbet^{+} B cells promote aberrant T_{FH} differentiation and affinity-based germinal center selection in lupus

Wenqian Zhang[a,b,c,1], Huihui Zhang[a,b,c,1], Shujun Liu[a,b,c], Fucan Xia[a,b,c], Zijian Kang[d], Yan Zhang[a,b,c], Yaoyang Liu[d], Hui Xiao[e], Lei Chen[a,b,c], Chuanxin Huang[a,b,c], Nan Shen[f], Huji Xu[d], and Fubin Li[a,b,c,2]

[a]Shanghai Institute of Immunology, Shanghai Jiao Tong University School of Medicine, 200025 Shanghai, China; [b]Faculty of Basic Medicine, Shanghai Jiao Tong University School of Medicine, 200025 Shanghai, China; [c]Key Laboratory of Cell Differentiation and Apoptosis of Chinese Ministry of Education, Shanghai Jiao Tong University School of Medicine, 200025 Shanghai, China; [d]Department of Rheumatology and Immunology, Shanghai Changzheng Hospital, Second Military Medical University, 200003 Shanghai, China; [e]Key Laboratory of Molecular Virology and Immunology, Vaccine Center, Institut Pasteur of Shanghai, Chinese Academy of Sciences, 200031 Shanghai, China; and [f]Shanghai Institute of Rheumatology, Renji Hospital, School of Medicine, Shanghai Jiao Tong University, 200001 Shanghai, China

Edited by Joe Craft, Yale University School of Medicine, New Haven, CT, and accepted by Editorial Board Member Ruslan Medzhitov August 5, 2019 (received for review February 25, 2019)

Excessive self-reactive and inadequate affinity-matured antigen-specific antibody responses have been reported to coexist in lupus, with elusive cellular and molecular mechanisms. Here, we report that the antigen-specific germinal center (GC) response–a process critical for antibody affinity maturation–is compromised in murine lupus models. Importantly, this defect can be triggered by excessive autoimmunity-relevant CD11c^{+}Tbet^{+} age-associated B cells (ABCs). In B cell-intrinsic Ship-deficient (ShipΔB) lupus mice, excessive CD11c^{+}Tbet^{+} ABCs induce deregulated follicular T-helper (T_{FH}) cell differentiation through their potent antigen-presenting function and consequently compromise affinity-based GC selection. Excessive CD11c^{+}Tbet^{+} ABCs and deregulated T_{FH} cell are also present in other lupus models and patients. Further, over-activated Toll-like receptor signaling in Ship-deficient B cells is critical for CD11c^{+}Tbet^{+} ABC differentiation, and blocking CD11c^{+}Tbet^{+} ABC differentiation in ShipΔB mice by ablating MyD88 normalizes T_{FH} cell differentiation and rescues antigen-specific GC responses, as well as prevents autoantibody production. Our study suggests that excessive CD11c^{+}Tbet^{+} ABCs not only contribute significantly to autoantibody production but also compromise antigen-specific GC B-cell responses and antibody-affinity maturation, providing a cellular link between the coexisting autoantibodies and inadequate affinity-matured antigen-specific antibodies in lupus models and a potential target for treating lupus.

lupus | CD11c^{+}T-bet^{+} B cells | germinal center selection | autoantibody | MyD88

The humoral immune system can efficiently select, from a large repertoire of B cells, for those of no/low affinity to self-antigens and high affinity to foreign antigens to produce antibodies, so that invading pathogens can be eliminated without self-harming (1, 2). Failure in these selections can lead to 2 distinct types of humoral immune defects featured by excessive self-reactive and inadequate affinity-matured antigen-specific antibody responses, respectively (3). Interestingly, several murine lupus models produce excessive autoantibodies and inadequate affinity-matured antigen-specific antibodies at the same time, including pristane (tetramethylpentadecane [TMPD])-induced lupus mice (4), mice with lupus-like chronic graft-versus-host disease (cGVHD) (5), and B cell-intrinsic Ship-deficient ($Ship^{\Delta B}$) mice with spontaneous lupus phenotypes (6). Lupus and lupus-like cGVHD patients have also been reported to respond less efficiently to vaccinations (7–9) and are more susceptible to infections (10–13). These observations raise the possibility that, in addition to impaired selection against self-reactive B cells, the selection for affinity-matured antigen-specific B cells is also impaired in lupus and lupus-like diseases.

The selection for affinity-matured antigen-specific B cells occurs in germinal centers (GCs), where B-cell receptors (BCRs) are rapidly diversified by somatic hypermutation (SHM) and selected by follicular T helper (T_{FH}) cells based on specificity and affinity, a process referred to as antibody affinity maturation (AAM) (14–16). Efficient AAM is critical for the development of protective antibodies against life-threating infectious pathogens, such as HIV and influenza viruses (17, 18). A prevailing model of this process involves BCR affinity-based uptake of antigens, which determine the amount of major histocompatibility complex (MHC) II antigen–peptide complexes presented by germinal center B (GCB) cells to cognate T_{FH} cells, and therefore the levels of survival signals T_{FH} cells provide to GCB cells (14–16). GCB cells with impaired SHM machinery or

Significance

The paradoxical coexistence of excessive autoantibodies and inadequate affinity-matured pathogen-specific antibodies in lupus is poorly understood. Here, we found that excessive CD11c^{+}T-bet^{+} age-associated B cells (ABCs)—a recently described autoimmunity-relevant B cell subset [K. Rubtsova *et al.*, *J. Clin. Invest.* 127, 1392–1404 (2017)]—not only contribute to the production of autoantibodies but also promote aberrant follicular T-helper (T_{FH}) cell differentiation and consequently compromise affinity-based germinal center (GC) B-cell selection and antibody-affinity maturation in lupus mouse models. Importantly, ablating B cell-intrinsic Toll-like receptor (TLR) signaling adaptor MyD88 in lupus mice inhibited CD11c^{+}T-bet^{+} ABC differentiation, normalized T_{FH} differentiation, and rescued GC selection, as well as prevented autoantibody production, suggesting that CD11c^{+}T-bet^{+} ABCs and TLR signaling are potential targets for lupus treatment.

Author contributions: W.Z., H.Z., Y.L., H. Xu, and F.L. designed research; W.Z., H.Z., S.L., F.X., Z.K., Y.Z., and F.L. performed research; H. Xiao, L.C., C.H., N.S., H. Xu, and F.L. contributed new reagents/analytic tools; W.Z., H.Z., S.L., F.X., C.H., and F.L. analyzed data; W.Z., H.Z., and F.L. wrote the paper; and F.L. provided funding.

The authors declare no conflict of interest.

This article is a PNAS Direct Submission. J.C. is a guest editor invited by the Editorial Board.

Data deposition: The RNA-seq data reported in this paper have been deposited in the National Center for Biotechnology Information Sequence Read Archive, https://www.ncbi.nlm.nih.gov/sra (accession no. PRJNA523485).

[1]W.Z. and H.Z. contributed equally to this work.

[2]To whom correspondence may be addressed. Email: fubin.li@sjtu.edu.cn.

This article contains supporting information online at www.pnas.org/lookup/suppl/doi:10.1073/pnas.1901340116/-/DCSupplemental.

Published online August 26, 2019.

negative selection signals, such as those with mutations in AID (19, 20) or Fas (21), have impaired AAM. The impaired AAM observed in Ship$^{\Delta B}$ mice is counterintuitive as Ship deficiency enhances not only AID expression but also negative selection (6, 22), raising the possibility of non-GCB cell-intrinsic mechanisms.

The number of T_{FH} cells has been proposed to set the threshold for GCB cell selection, and either inadequate or excessive T_{FH} cells may cause impaired GC selection and AAM (23, 24). Notably, excessive T_{FH} cells are also associated with autoantibody production and have been proposed to drive autoimmunity-associated spontaneous GC formation and extrafollicular B-cell responses (24, 25). Both mutations in T cells and myeloid antigen-presenting cells (APCs) have been shown to modulate T_{FH} differentiation (25–28). However, while T-B cognate interaction is critical for B-cell differentiation and several B cell-intrinsic factors (I-A^b, ICOSL, e.g.) have been shown to promote T_{FH} differentiation (29–31), the specific B-cell subsets responsible for such effect is not fully understood.

Age-associated B cell (ABC) is a B-cell subset recently identified independently by Hao et al. (32) and Rubtsov et al. (33), with a B220$^+$CD19$^+$CD43$^-$CD93$^-$CD23$^-$CD21$^-$CD11c$^+$Tbet$^+$ phenotype (34). The number of these cells increases when mice age, respond to intracellular infections or are under pathogenic conditions (34). ABCs have been implicated in autoimmunity in both mice and human (34). Several studies have shown that ABCs produce autoantibodies upon stimulation, and that inhibition of ABC differentiation by ablating Tbet prevents autoantibody production in mice (33–37), including our study in a lupus-like cGVHD model (35). In human, CD11c$^+$Tbet$^+$ B cells are linked to autoantibody-producing plasma cells (38). Toll-like receptor (TLR) agonists and BCR crosslinking, in addition to IFN-γ and IL-21 signalings, have been suggested to synergize to promote ABC differentiation (39, 40). Interestingly, B cell-intrinsic

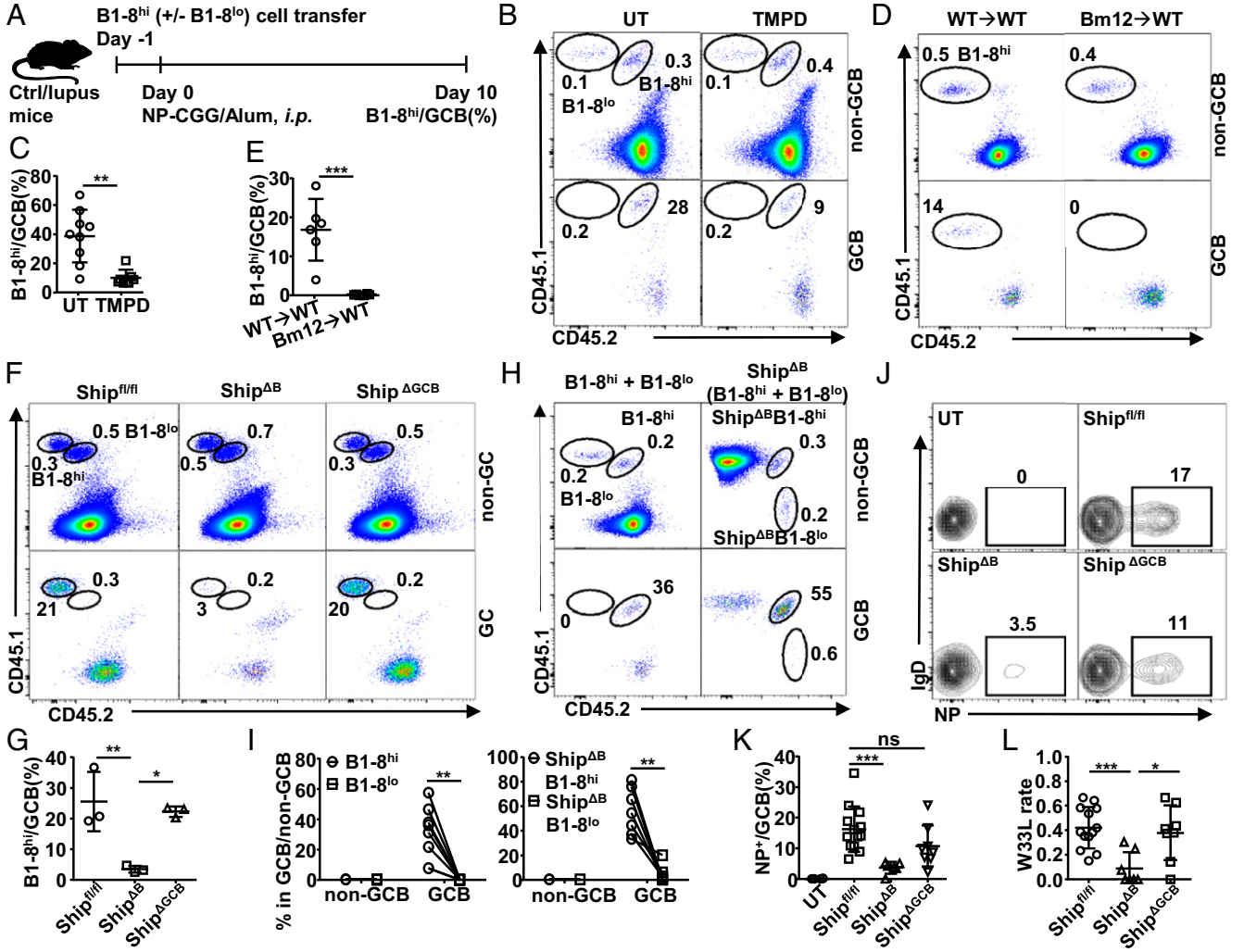

Fig. 1. GC selection is impaired in murine lupus models. (*A*) B1-8 cell transfer model for evaluating GC-selection efficiency. B1-8^{hi} cells were adoptively transferred into control or lupus mice on day −1 and quantified among GCB cells on day 10 after day 0 NP-CGG immunization. (*B–G*) Representative FACS profile (*B*, *D*, and *F*) and bar graph (*C*, *E*, and *G*) showing the percentage of B1-8^{hi} cells among non-GC or GC B cells in untreated or TMPD-treated mice (*B* and *C*), control or Bm12 cGVHD mice (*D* and *E*), Ship$^{fl/fl}$, Ship$^{\Delta B}$ (*Ship$^{fl/fl}$CD19-Cre$^+$*) or Ship$^{\Delta GCB}$ (*Ship$^{fl/fl}$Cg1-Cre$^+$*mice) (*F* and *G*) treated and analyzed as in *A*. (*H* and *I*) Representative FACS profile (*H*) and bar graph (*I*) showing the percentage of WT or Ship-deficient (Ship$^{\Delta B}$) B1-8^{hi} and B1-8^{low} cells among non-GC or GC B cells in WT mice treated and analyzed as in Fig. 1*A*. (*J* and *K*) Representative FACS profile (*J*) and bar graph (*K*) showing the percentage of NP-specific cells among GCB cells in untreated Ship$^{fl/fl}$ mice (UT) and Ship$^{fl/fl}$, Ship$^{\Delta B}$, or Ship$^{\Delta GCB}$ mice immunized with NP-CGG 2 wk earlier. (*L*) The W33L mutation rate of splenic V186.2–Cg1 transcripts in mice in *K*. Each symbol in the bar graphs represents data from an individual mouse. Bars represent means ± SD. *$P \le 0.05$; **$P \le 0.01$; ***$P \le 0.001$ (unpaired 2-tailed *t* test [*C* and *E*], 1-way ANOVA with Sidak's multiple comparisons test [*G*, *K*, and *L*], 2-way ANOVA with Sidak's multiple comparisons test [*I*]). A representative of 2 (*D* and *E*) or 3 (*B*, *C*, and *F–J*) independent experiments is shown; *K* and *L* are is summarized from multiple experiments with similar results.

TLR signaling adaptor MyD88 also regulates autoantibody production (41). But it is not clear whether ABCs mediate such regulation. Furthermore, ABCs can function as APCs (42), and its impact is not fully understood.

In this study, we investigated the cellular and molecular basis of the coexisting excessive autoantibodies and inadequate affinity-matured antigen-specific antibodies in lupus models and patients. We found that excessive $CD11c^{+}Tbet^{+}$ ABCs not only contribute to autoantibody production but also compromise antigen-specific GCB-cell responses and AAM in lupus models, and that blocking $CD11c^{+}Tbet^{+}$ ABC differentiation by ablating MyD88 rescues both these humoral immune defects.

Results

Antigen-Specific GCB-Cell Responses Are Impaired in Murine Lupus Models. To investigate AAM in lupus, we selected 3 established murine lupus models (*SI Appendix*, Fig. S1*A*): TMPD-induced model (43–45), Bm12 cGVHD model (35, 46, 47), and $Ship^{\Delta B}$ spontaneous lupus model (48–50) (all referred to "lupus models" in this study), which were all confirmed to produce anti–double-stranded DNA (dsDNA) autoantibodies (*SI Appendix*, Fig. S1*B*). Our investigation of AAM focused on antigen-specific GCB-cell differentiation and selection, given the reports of active SHM in these models and autoantibodies (6, 21, 51–53). The (4-hydroxy-3-nitrophenyl)acetyl (NP)-specific B1-8 B-cell system (54, 55) was exploited to evaluate the efficiency of GC selection for high-affinity antigen-specific B cells in a host (Fig. 1*A*). When NP-specific high-affinity $B1\text{-}8^{hi}$, alone or together with low-affinity $B1\text{-}8^{low}$ cells, were adoptively transferred into wild-type (WT) mice, $B1\text{-}8^{hi}$ cells dominated in GCB cells following NP immunization, but not in non-GCB cells (Fig. 1 *B* and *C*), as expected for efficient GC selection for high-affinity antigen-specific B cells based on the previous studies (54). In contrast, we observed a large decrease in the proportion of $B1\text{-}8^{hi}$ cells among GCB cells in TMPD-treated WT mice (treated with TMPD for 2 wk, representing the early stage of TMPD-induced lupus mice) (Fig. 1 *B* and *C*), suggesting impaired antigen-specific GC responses in these mice. In Bm12 cGVHD mice, more severe impairment was observed, with a complete loss of positive selection for $B1\text{-}8^{hi}$ cells in GC following NP immunization (Fig. 1 *D* and *E*), although more GCB cells were observed (*SI Appendix*, Fig. S1*C*).

We further investigated antigen-specific GC responses in $Ship^{\Delta B}$ ($Ship^{fl/fl}CD19\text{-}Cre^{+}$) mice (*SI Appendix*, Fig. S1*A*), where impaired AAM has been reported and attributed to Ship deficiency in GCB

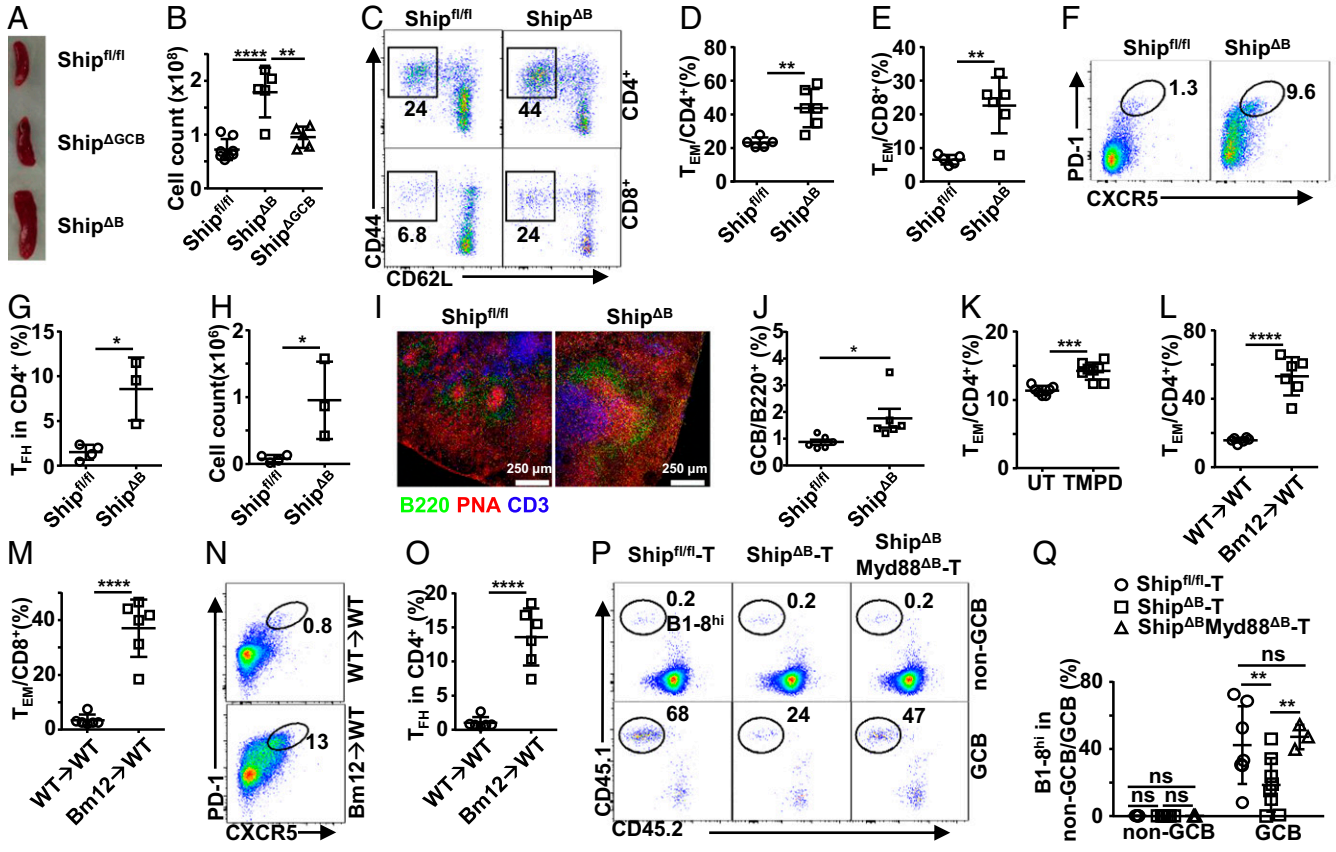

Fig. 2. Aberrant T-cell profile is responsible for impaired GC selection in lupus mice. (*A* and *B*) Representative image (*A*) and cell counts (*B*) of spleens from $Ship^{fl/fl}$, $Ship^{\Delta B}$, and $Ship^{\Delta GCB}$ mice. (*C*–*E*) Representative FACS profile (*C*) and bar graph (*D* and *E*) showing the percentage of $CD44^{+}CD62L^{-}$ effector/memory cells (T_{EM}) among $CD4^{+}$ (*D*) and $CD8^{+}$ (*E*) T cells in the spleen of $Ship^{fl/fl}$ and $Ship^{\Delta B}$ mice. (*F*–*H*) Representative FACS profile (*F*) and bar graph (*G* and *H*) showing the percentage (*F* and *G*) and absolute number (*H*) of T_{FH} cells in the spleen of $Ship^{fl/fl}$ and $Ship^{\Delta B}$ mice analyzed 2 wk after NP-CGG immunization. (*I*) Immunofluorescence image of frozen sections of spleens from $Ship^{fl/fl}$ mice and $Ship^{\Delta B}$ mice analyzed 2 wk after NP-CGG immunization. (*J*) Percentage of GCB cells ($PNA^{+}CD95^{+}$) in total spleen B cells of $Ship^{fl/fl}$ or $Ship^{\Delta B}$ mice. (*K*–*M*) Percentage of T_{EM} cells among $CD4^{+}$ (*K* and *L*) or $CD8^{+}$ (*M*) T cells in the spleen of TMPD-induced mice (*K*) and Bm12 cGVHD mice (*L* and *M*). (*N* and *O*) Representative FACS profile (*N*) and bar graph (*O*) showing the percentage of T_{FH} cells in the spleen of Bm12 cGVHD mice 2 wk after NP-CGG immunization. (*P* and *Q*) Representative FACS profile (*P*) and bar graph (*Q*) showing the percentage of $B1\text{-}8^{hi}$ cells among non-GC or GC B cells in T cell-deficient mice ($TCR\beta^{-/-}TCR\delta^{-/-}$) transplanted with T cells isolated from $Ship^{fl/fl}$, $Ship^{\Delta B}$, or $Ship^{\Delta B}Myd88^{\Delta B}$ mice and then treated and analyzed as in Fig. 1*A*. Each symbol in the bar graphs represents an individual mouse. Bars represent means ± SD. ns, not significant; $*P \le 0.05$; $**P \le 0.01$; $***P \le 0.001$; $****P \le 0.0001$ (1-way ANOVA with Sidak's multiple comparisons test [*B*]; unpaired 2-tailed *t* test [*D*, *G*, *H*, *J*–M, and *O*], 2-way ANOVA with Sidak's multiple comparisons test [*Q*]). A representative of 2 (*L*–*O*) or 3 (*A*–*K*) independent experiments is shown. *Q* is summarized from 2 independent experiments with similar results.

cells (6). Ship$^{\Delta B}$ mice were confirmed to have impaired GC selection for endogenous Ship-deficient NP-specific cells upon NP immunization (*SI Appendix*, Fig. S1 *D* and *E*), as well as impaired AAM, as shown by the reduced high-affinity V186.2-W33L mutation frequency (56) (*SI Appendix*, Fig. S1*F*). Interestingly, when evaluated in the B1-8^{hi} cell transfer model, as illustrated in Fig. 1*A*, Ship$^{\Delta B}$ mice displayed a severe defect in positively selecting Ship-sufficient B1-8^{hi} cells for GC responses (Fig. 1 *F* and *G*), suggesting that regardless of whether GCB cells have Ship deficiency, their selection in Ship$^{\Delta B}$ mice is impaired. Together, our data demonstrate that GC selection is profoundly impaired in both induced and spontaneous murine lupus models.

Ship Deficiency in GCB Cells Is Not Responsible for Impaired GC Selection in Ship$^{\Delta B}$ Mice. Given the impact of Ship on B-cell activation and survival (22), we further investigated whether Ship deficiency in GCB cells is responsible for the compromised GC selection in Ship$^{\Delta B}$ mice. Ship-deficient B1-8^{hi} and B1-8^{lo} B cells (Ship$^{\Delta B}$B1-8^{hi} and Ship$^{\Delta B}$B1-8^{lo}, respectively) were generated and used to test whether Ship deficiency can overwrite BCR affinity-based GCB-cell selection. As shown in Fig. 1 *H* and *I*, Ship$^{\Delta B}$ B1-8^{hi} cells outcompete Ship$^{\Delta B}$B1-8^{lo} cells in GC responses, similarly as B1-8^{hi} cells outcompete B1-8^{lo} cells, suggesting that BCR affinity-based GC selection is not compromised in Ship-deficient GCB cells.

This notion was further tested in GCB-specific Ship-conditional knockout mice driven by Cγ1-Cre (57) (*Ship$^{fl/fl}$Cg1-Cre^{+}*, or Ship$^{\Delta GCB}$), which have comparably efficient Ship deletion as Ship$^{\Delta B}$ mice in GCB cells, but not in other B cells or non-B cells (*SI Appendix*, Fig. S2 *A–C*). In contrast to Ship$^{\Delta B}$ mice, Ship$^{\Delta GCB}$ mice have a largely normal percentage of endogenous NP-specific GCB cells (Fig. 1 *J* and *K*) and a normal frequency of high-affinity NP-specific V186.2-W33L mutations in NP-specific GC responses (Fig. 1*L*), suggesting that Ship-deficient, endogenous NP-specific GCB cells have no defect in participating GC responses and undergoing proper AAM. In the B1-8^{hi} cell transfer model, Ship$^{\Delta GCB}$ mice also displayed normal NP-specific GC responses (Fig. 1 *F* and *G*). Together, these results suggest that the observed GC selection defect in Ship$^{\Delta B}$ mice is not due to the direct impact of Ship deficiency on GCB cells, but rather to its impact on other B-lineage cells that may regulate GC responses indirectly.

Aberrant T-Cell Profile Is Responsible for Impaired GC Selection in Lupus Mice. To characterize the factors responsible for the impaired GC selection in Ship$^{\Delta B}$ mice, we analyzed their T-cell profiles, given that T$_{FH}$ cells have been demonstrated to regulate GCB-cell selection directly (24, 58, 59). Ship$^{\Delta B}$ mice have large spleens with increased numbers of splenocytes (Fig. 2 *A* and *B*) and an aberrantly activated T-cell profile with increased percentages of CD44^{+}CD62L^{-} effector/memory T (T$_{EM}$) cells among both CD4^{+} and CD8^{+} T cells (Fig. 2 *C–E*). Notably, we observed a large increase in T$_{FH}$ cells by flow cytometry (Fig. 2 *F–H*). Consistently, there appear to be more T cells colocalizing with GC (Fig. 2*I* and *SI Appendix*, Fig. S3*A*) and more spontaneous GCs in Ship$^{\Delta B}$ mice (Fig. 2*J* and *SI Appendix*, Fig. S3*B*). We also observed increased T$_{EM}$ cells in TMPD-treated mice (Fig. 2*K* and *SI Appendix*, Fig. S3*C*) and Bm12 cGVHD mice (Fig. 2 *L* and *M* and *SI Appendix*, Fig. S3*D*) and excessive T$_{FH}$ cells in Bm12 cGVHD mice (Fig. 2 *N* and *O*), suggesting that aberrant T-cell activation and T$_{FH}$-cell accumulation are common features of these models.

To test whether the aberrant T-cell profile (with increased T-cell activation and T$_{FH}$-cell accumulation) is responsible for the impaired GC selection in these models, we adoptively transferred pan-T cells isolated from Ship$^{\Delta B}$ mice into T cell-deficient mice (*TCRβ$^{-/-}$ TCRδ$^{-/-}$*) and evaluated GC-selection efficiency in these recipients using the B1-8^{hi} cell transfer model. As shown in Fig. 2 *P* and *Q*, T cells isolated from Ship$^{\Delta B}$ mice are significantly less efficient, as compared with those from WT mice, in supporting the selection of B1-8^{hi} cells for NP-specific GC responses. These data suggest that the aberrant T-cell profile featuring increased activation and T$_{FH}$-cell accumulation is responsible for the observed GC selection defect in our lupus models.

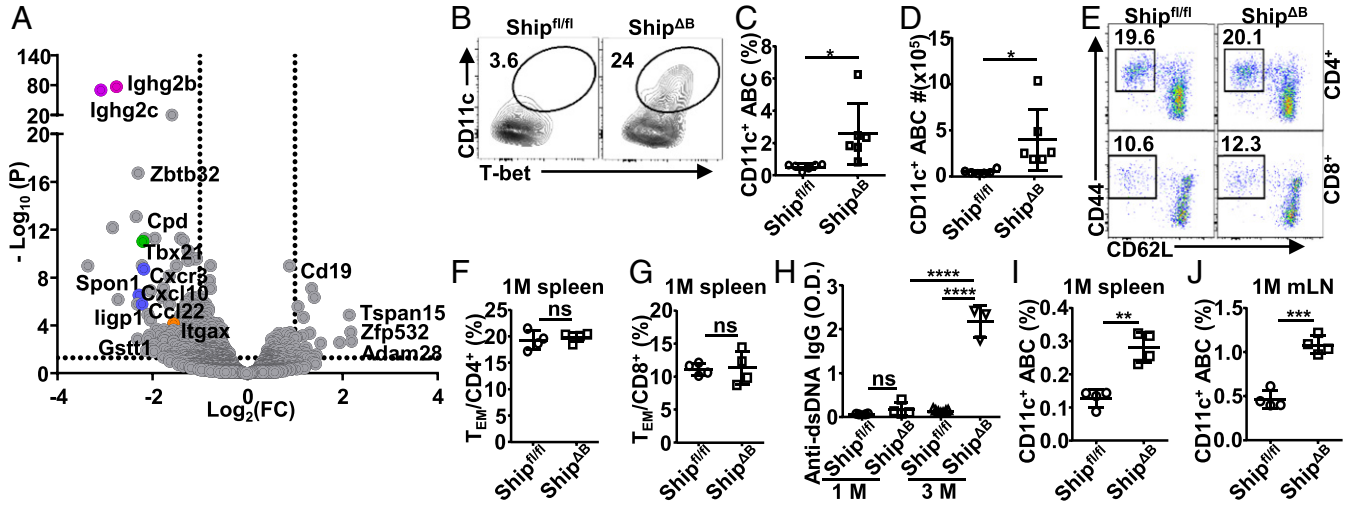

Fig. 3. Excessive CD11c^{+}Tbet^{+} ABCs precede aberrant T-cell activation. (*A*) Volcano plot showing genes expressed differentially (change in expression of over 2-fold) in B-lineage cells (sorted as B220^{+} and B220^{low}CD138^{hi}) from Ship$^{fl/fl}$ mice relative to those from Ship$^{\Delta B}$ mice. (*B–D*) Frequency of CD11c^{+}Tbet^{+}ABCs among B220^{+}CD19^{+}CD43^{-}CD93^{-}CD23^{-}CD21^{-} cells (*B*), B220^{+}CD19^{+} cells (*C*), and absolute cell number of CD11c^{+}Tbet^{+}ABC per spleen (*D*) of Ship$^{fl/fl}$ and Ship$^{\Delta B}$ mice (3 to ∼4 mo old). (*E–G*) Representative FACS profile (*E*) and bar graph (*F* and *G*) showing the percentage of CD44^{+}CD62L^{-} effector/memory cells (T$_{EM}$) among CD4^{+} (*E* and *F*) and CD8^{+} (*E* and *G*) T cells in the spleen of 1-mo-old Ship$^{fl/fl}$ and Ship$^{\Delta B}$ mice. (*H*) Anti-dsDNA IgG autoantibody levels in the serum of Ship$^{fl/fl}$ and Ship$^{\Delta B}$ mice at the age of 1 or 3 mo. (*I* and *J*) Percentage of CD11c^{+} ABCs among B cells in the spleen (*I*) or mesenteric lymph node (mLN) (*J*) of 1-mo-old Ship$^{fl/fl}$ and Ship$^{\Delta B}$ mice. Each symbol in the bar graphs represents an individual mouse. Bars represent means ± SD. ns, not significant; *$P \le 0.05$; **$P \le 0.01$; ***$P \le 0.001$; ****$P \le 0.0001$ (unpaired 2-tailed *t* test [*C*, *D*, *F*, *G*, *I*, and *J*], 1-way ANOVA with Sidak's multiple comparisons test [*H*]). A representative of 3 independent experiments is shown (*B–J*).

Excessive CD11c$^+$Tbet$^+$ Age-Associated B Cells Precede Aberrant T-Cell Activation and Autoantibody Production in Ship$^{\Delta B}$ Mice. To study how B cell-intrinsic Ship deficiency causes impaired GC selection, we investigated the responsible B-lineage cell subsets. Since Ship$^{\Delta GCB}$ mice have efficient Ship deletion in GCB cells (*SI Appendix*, Fig. S2 *A–C*) and normal GC selection (Fig. 1 *F*, *G*, *J*, and *K*), we reasoned that the responsible B-lineage cells are not likely GC or post-GC B cells. Ship$^{\Delta B}$ mice have been reported and confirmed to have normal B-cell development in the bone marrow (6). In the periphery, despite of increased number of splenic B cells in Ship$^{\Delta B}$ mice (*SI Appendix*, Fig. S4*A*), most B-cell subsets have either no or only minor changes in their proportions among B-lineage cells, including transitional B cells (CD93$^+$), follicular B (FOB) cells, marginal zone (MZ) B cells, B1-a, B1-b, and regulatory B (Breg) cells (*SI Appendix*, Fig. S4*B*). In transcriptome analysis, Ship$^{\Delta B}$ B splenic B-lineage cells (B220$^+$ and B220^{low}CD138^{hi} cells) displayed significantly increased expression of immunoglobulin (Ig) genes (*SI Appendix*, Fig. S4*C*) and hallmarks related to immune activation (*SI Appendix*, Fig. S4*D*). Interestingly, among genes with the most significantly increased expression in Ship$^{\Delta B}$ B cells (Fig. 3*A*), both *Itgax* (encoding CD11c) and *Tbx21*(encoding Tbet) are markers of the recently described CD11c$^+$Tbet$^+$ ABCs (34), suggesting increased CD11c$^+$Tbet$^+$ ABCs in Ship$^{\Delta B}$ mice. ABCs were identified as B220$^+$CD19$^+$CD93$^-$CD43$^-$CD21$^-$CD23$^-$ cells, among which CD11c$^+$Tbet$^+$ cells were further gated as CD11c$^+$Tbet$^+$ ABCs (*SI Appendix*, Fig. S4*E*) or CD11c$^+$ ABCs since Tbet is specifically expressed in the majority of CD11c$^+$ ABCs (Fig. 3*B* and *SI Appendix*, Fig. S4 *E* and *F*). In adult Ship$^{\Delta B}$ mice, we observed ~5-fold more CD11c$^+$ ABCs among B-lineage cells (Fig. 3 *B–D*). Notably, in 1-mo-old Ship$^{\Delta B}$ mice, we observed neither aberrant T-cell activation (Fig. 3 *E–G*) nor significant autoantibody production (Fig. 3*H*), but significantly more CD11c$^+$ ABCs in both spleen and lymph nodes (Fig. 3 *I* and *J*). These results suggest that the observed excessive CD11c$^+$ ABCs are not secondary to either aberrant T-cell activation or autoantibody production in Ship$^{\Delta B}$ mice.

Excessive CD11c$^+$Tbet$^+$ ABCs Promote Deregulated T-Cell Differentiation with T$_{FH}$ Phenotypes through Their Potent Antigen-Presenting Function. Since CD11c$^+$Tbet$^+$ ABCs have APC function (42), we hypothesized that excessive CD11c$^+$Tbet$^+$ ABCs promote aberrant T-cell activation and T$_{FH}$ differentiation in lupus mice through their APC function. Pan-B cells can efficiently prime OVA-specific OT-II T cells in the presence of OVA peptide antigen, as indicated by the

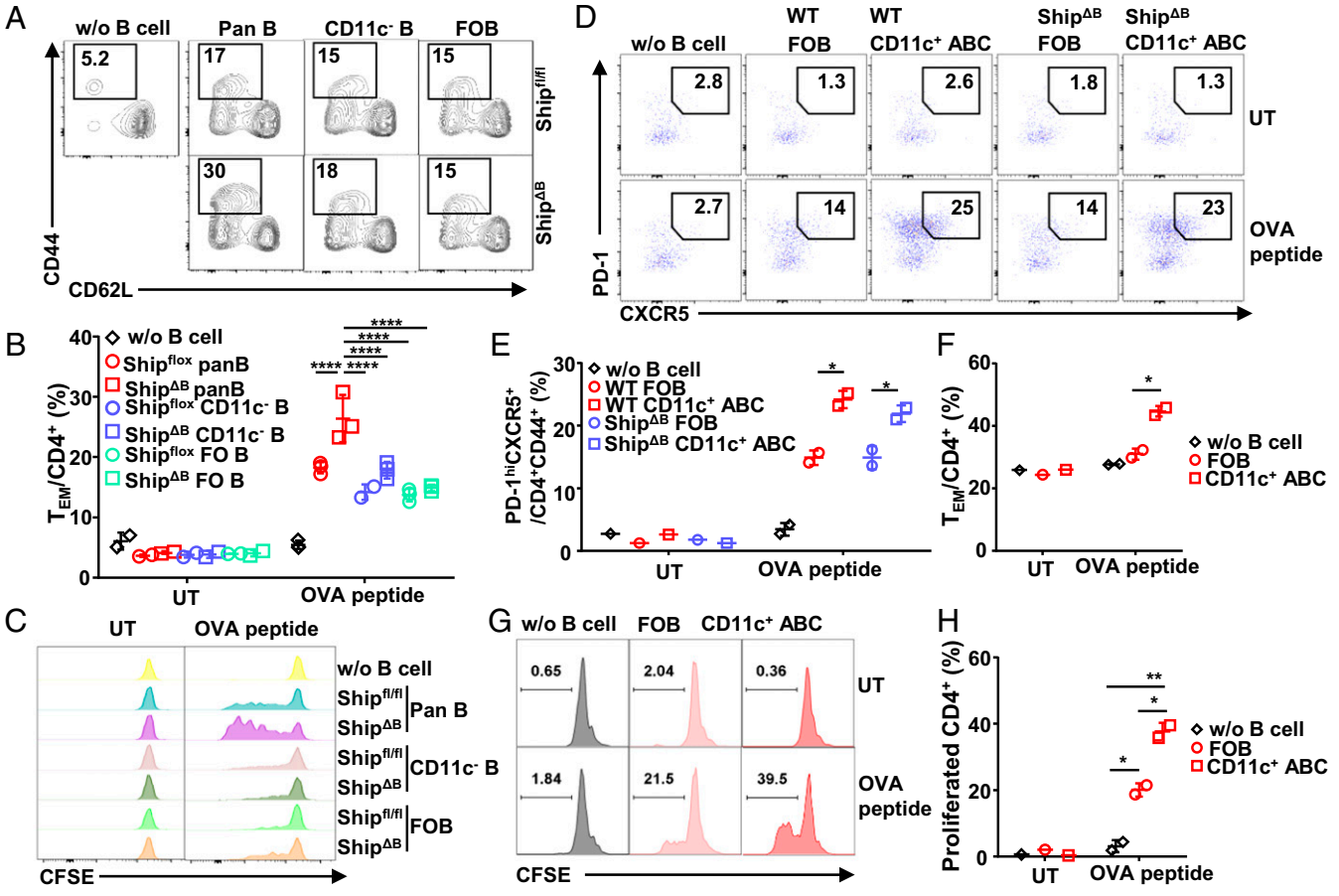

Fig. 4. CD11c$^+$Tbet$^+$ ABCs promote T-cell differentiation with T$_{FH}$ phenotypes through antigen-presenting function. (*A* and *B*) Representative FACS profile (*A*) and bar graph (*B*) showing the percentage of CD44$^+$CD62L$^-$ effector/memory cells (T$_{EM}$) among carboxyfluorescein succinimidyl ester (CFSE)-labeled OT-II T cells primed by Ship$^{fl/fl}$ or Ship$^{\Delta B}$ pan-B, CD11c$^-$ B, or FOB cells in the presence (*A* and *B*) or absence (UT) (*B*) of OVA peptide (1 μg/mL) for 36 h. (*C*) Representative FACS profile showing the CFSE levels of OT-II T cells primed as in *A* and *B* with indicated B-cell subsets in the absence (UT) or presence of 0.3 μg/mL of OVA peptide for 84 h. (*D* and *E*) Representative FACS profile (*D*) and bar graph (*E*) showing the percentage of PD-1^{hi}CXCR5$^+$ cells among activated (CD4$^+$CD44$^+$) OT-II cells primed by WT (Bm12 cGVHD lupus mice) or Ship$^{\Delta B}$ FOB or CD11c$^+$ ABCs in the absence (UT) or presence of OVA peptide (1 μg/mL) for 72 h. (*F*) Percentage of T$_{EM}$ cells among OT-II T cells treated as in *D* and *E*. (*G–H*) Representative FACS profile showing the CFSE levels (*G*) and bar graph showing the percentage of cells proliferated more than twice (*H*) among OT-II T cells primed by WT FOB or CD11c$^+$ ABCs as in *D*. Bars represent means ± SD. *$P \leq 0.05$; **$P \leq 0.01$; ****$P \leq 0.0001$ (2-way ANOVA with Sidak's multiple comparisons test [*B* and *H*], unpaired 2-tailed *t* test [*E* and *F*]). A representative of 3 independent experiments is shown.

significantly increased percentage of $CD44^+CD62L^-$ cells (Fig. 4 *A* and *B*) and proliferation (Fig. 4*C*). When compared with WT cells, $Ship^{\Delta B}$ pan-B cells are significantly more potent in inducing OT-II T-cell activation in an antigen-dependent manner (Fig. 4 *A*–*C*). However, this increased potency is not due to Ship deficiency in FOB cells, as purified $Ship^{\Delta B}$ and WT FOB cells have the same potencies in inducing OT-II T-cell activation (Fig. 4 *A*–*C*). In contrast, depleting $CD11c^+$ cells from pan-B cells removed the extra potency of $Ship^{\Delta B}$ pan-B cells over WT cells and resulted in comparable potencies similar to those of FOB cells (Fig. 4 *A*–*C*). $CD11c^+$ ABCs purified from $Ship^{\Delta B}$ mice were also directly analyzed and confirmed to be more potent than FOB cells in priming OT-II T cells in an antigen-dependent manner (Fig. 4 *D* and *E*). These data suggest that $CD11c^+$ B cells are responsible for the increased T-cell activation induced by $Ship^{\Delta B}$ pan-B cells.

Notably, increased PD-1 and CXCR5 expression, phenotypes of T_{FH} cells, was observed in $Ship^{\Delta B}$ $CD11c^+$ ABC-primed T cells (Fig. 4 *D* and *E*). WT $CD11c^+$ ABCs purified from Bm12 cGVHD lupus mice also displayed superior activity over FOB cells in inducing OT-II cell activation, proliferation (Fig. 4 *F*–*H*), and differentiation into activated T cells with increased PD-1 and CXCR5 expression (Fig. 4 *D* and *E*). These data suggest that excessive $CD11c^+Tbet^+$ ABCs can promote deregulated T-cell differentiation with T_{FH} phenotypes through their potent antigen-presenting function in lupus mice. It is further confirmed that $CD11c^+$ ABCs express higher levels of MHC II (*SI Appendix*, Fig. S5*A*) and present more antigen (*SI Appendix*, Fig. S5 *B* and *C*).

Deregulated TLR and BCR Signalings Accelerate Ship-Deficient $CD11c^+$ ABC Differentiation. To investigate how Ship deficiency leads to excessive $CD11c^+Tbet^+$ ABCs in $Ship^{\Delta B}$ mice, we analyzed proliferation and apoptosis of Ship-deficient and sufficient $CD11c^+Tbet^+$ ABCs and observed no significant differences (Fig. 5 *A* and *B*), suggesting that excessive $CD11c^+Tbet^+$ ABCs are results of increased differentiation. Previous studies have shown that FOB cells can differentiate into $CD11c^+$ B cells in vitro upon TLR7 ligand and IL-21 stimulation (39). In this in vitro system, we found that Ship-deficient FOB cells can differentiate into $CD11c^+$ cells much more efficiently than WT FOB cells (Fig. 5 *C* and *D*).

Given the negative impact of Ship on TLR signaling in myeloid cells (60–62), we tested whether Ship inhibits $CD11c^+$ B-cell differentiation by inhibiting TLR signaling. As shown in Fig. 5*E*, CL097 induced stronger IκBα phosphorylation in $Ship^{\Delta B}$ B cells than in WT B cells, suggesting that TLR7 signal (63) is enhanced

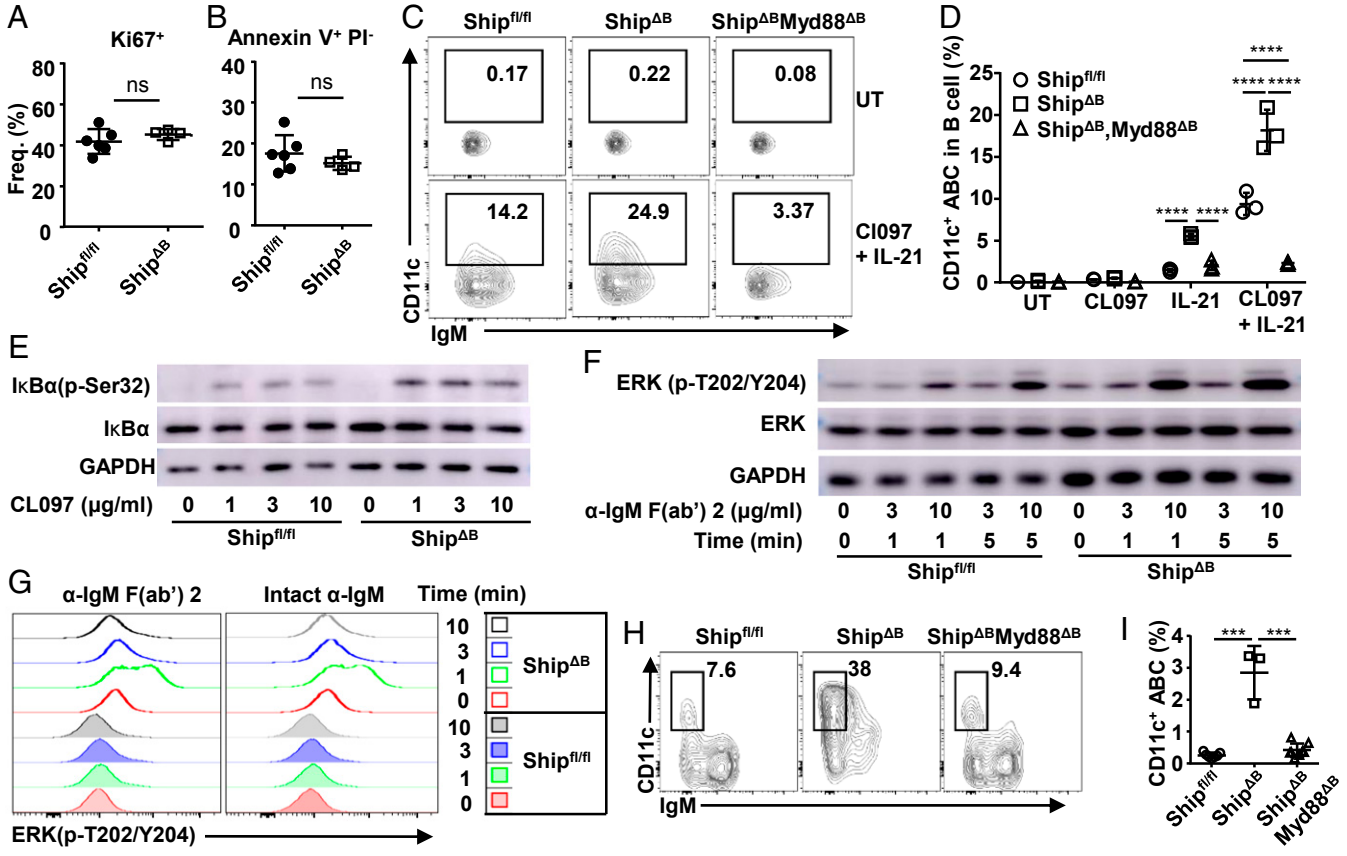

Fig. 5. Ship deficiency accelerates $CD11c^+$ ABC differentiation. (*A* and *B*) Percentage of $Ki67^+$ (*A*) cells and Annexin V^+PI^- (*B*) cells among splenic $CD11c^+$ ABCs in $Ship^{fl/fl}$ and $Ship^{\Delta B}$ mice. (*C* and *D*) Representative FACS profile (*C*) and bar graph (*D*) showing the percentage of $CD11c^+$ cells among FOB cells isolated from $Ship^{fl/fl}$, $Ship^{\Delta B}$, or $Ship^{\Delta B}Myd88^{\Delta B}$ mice and cultured for 48 h in the absence (UT) or presence of TLR7 ligand CL097, IL-21, or their combination. Each symbol in the bar graphs represents an individual mouse (*A* and *B*) or tissue-culture sample (*D*). (*E*) IκBα phosphorylation levels in FOB cells isolated from $Ship^{fl/fl}$ or $Ship^{\Delta B}$ mice and treated with the indicated concentrations of CL097 for 10 min. (*F*) ERK1/2 phosphorylation levels in FOB cells isolated from $Ship^{fl/fl}$ or $Ship^{\Delta B}$ mice and treated with the indicated concentrations of αIgM $(Fab)_2'$ for 1 or 5 min. (*G*) Representative FACS profile showing ERK1/2 phosphorylation levels in FOB cells among $Ship^{fl/fl}$ or $Ship^{\Delta B}$ splenocytes treated with 10 μg/mL αIgM $(Fab)_2'$ or intact anti-IgM for the indicated time intervals. (*H* and *I*) Representative FACS profile (*H*) and bar graph (*I*) showing the percentage of $CD11c^+$ ABCs among B cells in the spleen of $Ship^{fl/fl}$, $Ship^{\Delta B}$, and $Ship^{\Delta B}Myd88^{\Delta B}$ mice. Each symbol in the bar graphs represents an individual mouse. Bars represent means ± SD. ns, not significant; $^{***}P \le 0.001$; $^{****}P \le 0.0001$ (unpaired 2-tailed *t* test [*A* and *B*], 2-way ANOVA with Sidak's multiple comparisons test [*D*], 1-way ANOVA with Sidak's multiple comparisons test [*I*]). A representative of 3 independent experiments is shown.

in Ship-deficient B cells. Since BCR signaling also promotes CD11c$^+$ B-cell differentiation, we confirmed previous reports that Ship negatively regulates BCR signals, as shown by increased ERK phosphorylation in anti-IgM–treated Ship$^{\Delta B}$ FOB cells (Fig. 5 *F* and *G*). These data suggest that Ship can inhibit TLR and BCR signalings and therefore restrict CD11c$^+$ ABC differentiation.

We further investigated the impact of ablating TLR-signaling adaptor MyD88 (64) on CD11c$^+$ ABC differentiation and found that ablating MyD88 almost completely blocked Ship-deficient FOB cells to differentiate into CD11c$^+$ B cells in vitro (Fig. 5 *C* and *D*). Furthermore, deletion of B cell-intrinsic MyD88 in Ship$^{\Delta B}$ mice restored CD11c$^+$ ABCs levels (Fig. 5 *H* and *I*), further supporting a critical role of TLR signals, mediated by MyD88 and inhibited by Ship, in CD11c$^+$ ABC differentiation.

Inhibition of CD11c$^+$Tbet$^+$ ABC Differentiation by Ablating MyD88 Prevents Aberrant T$_{FH}$ Differentiation and Restores Antigen-Specific GC Responses in Ship$^{\Delta B}$ Mice. We further investigated whether inhibition of CD11c$^+$Tbet$^+$ ABC differentiation by ablating MyD88 can rescue the GC selection defect in Ship$^{\Delta B}$ mice. As shown in Fig. 6 *A* and *B*, the T-cell activation profile is normalized in Ship$^{\Delta B}$ Myd88$^{\Delta B}$ mice, as well as T$_{FH}$ differentiation (Fig. 6 *C*–*E*). Pan-T cells isolated from Ship$^{\Delta B}$Myd88$^{\Delta B}$ mice, when transferred into T cell-deficient mice, support the efficient selection of B1-8^{hi} cells in NP-specific GC responses (Fig. 2 *P* and *Q*). In the B1-8^{hi} transfer model, Ship$^{\Delta B}$Myd88$^{\Delta B}$ mice are equally efficient as WT mice in selecting B1-8^{hi} cells for NP-specific GC responses (Fig. 6 *F* and *G*). Furthermore, unlike in Ship$^{\Delta B}$ mice, endogenous NP-specific B cells were also efficiently selected into the GCB-cell compartment in Ship$^{\Delta B}$Myd88$^{\Delta B}$ mice upon NP immunizations (Fig. 6 *H* and *I*), and the frequency of the high-affinity V186.2-W33L mutation was restored to normal levels in Ship$^{\Delta B}$Myd88$^{\Delta B}$ mice (Fig. 6*J*), suggesting normal GC selection and AAM in these mice. Notably, normal NP-specific GC responses and AAM were observed in Myd88$^{\Delta B}$ mice (Fig. 6 *H*–*J*), suggesting that ablating MyD88 in GCB cells does not significantly change the NP-specific GC responses in our model. Together, these data suggest that inhibiting CD11c$^+$ B-cell differentiation in Ship$^{\Delta B}$ mice by ablating B cell-intrinsic TLR-MyD88 signaling not only prevents aberrant T-cell activation and T$_{FH}$ differentiation but also rescues GC selection and AAM.

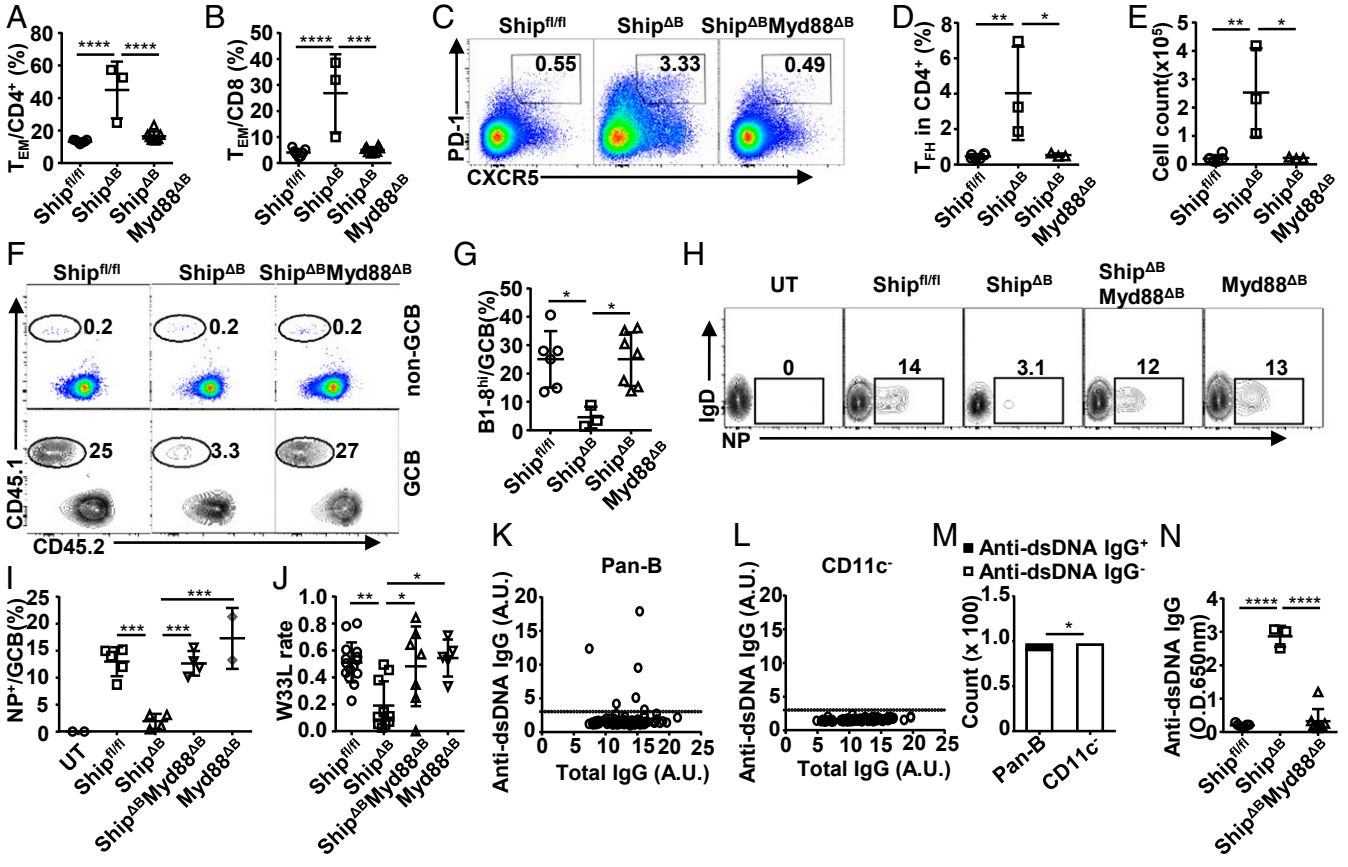

Fig. 6. Inhibition of CD11c$^+$Tbet$^+$ ABC differentiation by ablating MyD88 prevents aberrant T$_{FH}$ differentiation and restores antigen-specific GC responses in Ship$^{\Delta B}$ mice. (*A* and *B*) The percentage of T$_{EM}$ cells among CD4$^+$ (*A*) or CD8$^+$ (*B*) T cells in the spleen of Ship$^{fl/fl}$, Ship$^{\Delta B}$, and Ship$^{\Delta B}$Myd88$^{\Delta B}$ mice. (*C*–*E*) Representative FACS profile (*C*) and bar graph (*D* and *E*) showing the percentage (*C* and *D*) and absolute number (*E*) of T$_{FH}$ cells in the spleen of Ship$^{fl/fl}$, Ship$^{\Delta B}$, and Ship$^{\Delta B}$Myd88$^{\Delta B}$ mice. (*F* and *G*) Representative FACS profile (*F*) and bar graph (*G*) showing the percentage of B1-8^{hi} cells among non-GC and GC B cells in Ship$^{fl/fl}$, Ship$^{\Delta B}$, and Ship$^{\Delta B}$Myd88$^{\Delta B}$ mice treated and analyzed as in Fig. 1*A*. (*H* and *I*) Representative FACS profile (*H*) and bar graph (*I*) showing the percentage of NP-specific cells among GCB cells in untreated Ship$^{fl/fl}$ mice (UT) and Ship$^{fl/fl}$, Ship$^{\Delta B}$, Ship$^{\Delta B}$Myd88$^{\Delta B}$, or Myd88$^{\Delta B}$ mice immunized with NP-CGG 2 wk earlier. (*J*) W33L rate of splenic V186.2–Cg1 transcripts in mice treated as in *H* and *I*. (*K* and *L*) Anti-dsDNA IgG levels produced by Ship$^{\Delta B}$ splenic pan-B or CD11c$^-$ B cells cocultured with NB-21.2D9 feeder cells for 10 d (100 B cells per well), quantified as the ratio of signal to noise (S/N), with S/N $\geq$ 3 (marked by dotted lines) considered as anti-dsDNA IgG$^+$ samples and otherwise anti-dsDNA IgG$^-$ samples. (*M*) Bar graph showing the number of anti-dsDNA IgG$^+$ and anti-dsDNA IgG$^-$ samples in *K* and *L*. (*N*) Anti-dsDNA IgG autoantibody levels in Ship$^{\Delta B}$ and Ship$^{\Delta B}$Myd88$^{\Delta B}$ mice. Each symbol in the bar graphs represents an individual mouse. Bars represent means $\pm$ SD. *$P \leq 0.05$; **$P \leq 0.01$; ***$P \leq 0.001$; ****$P \leq 0.0001$ (1-way ANOVA with Sidak's multiple comparisons test [*A*, *B*, *D*, *E*, *G*, *I*, *J*, and *N*], χ^2 test [*M*]). A representative of 2 (*K*–*M*) or 3 independent experiments (*A*–*I* and *N*) is shown. *J* is summarized from multiple experiments with similar results.

CD11c$^+$Tbet$^+$ ABCs Contribute Significantly to Autoantibody Production in Ship$^{\Delta B}$ Mice. To investigate whether CD11c$^+$Tbet$^+$ ABCs cells contribute to autoantibody production, their ability to produce anti-dsDNA autoantibody was analyzed. We found that depleting CD11c$^+$ cells from Ship$^{\Delta B}$ pan-B cells also depleted anti-dsDNA autoantibody-producing B cells (Fig. 6 *K–M*), suggesting that CD11c$^+$ B cells are primarily responsible for anti-dsDNA autoantibody production in Ship$^{\Delta B}$ mice. Notably, no significant autoantibody production was observed in Ship$^{\Delta B}$Myd88$^{\Delta B}$ mice (Fig. 6*N*), suggesting that inhibiting CD11c$^+$Tbet$^+$ ABC differentiation in Ship$^{\Delta B}$ mice also prevents autoantibody production. Together, these data suggest that CD11c$^+$Tbet$^+$ ABCs are critical for the observed autoantibody production in Ship$^{\Delta B}$ lupus mice.

The Maintenance of T_{FH} Responses Requires CD11c$^+$ Cells. We also analyzed the levels of CD11c$^+$Tbet$^+$ ABCs in TMPD-induced and Bm12 cGVHD models and found significantly increased CD11c$^+$Tbet$^+$ ABCs in both models, but at different levels (Fig. 7 *A* and *B*). These data suggest that excessive CD11c$^+$ B cells are a common feature in murine lupus models.

It has been shown that dendritic cells are critical for the initial priming and commitment of T_{FH} cells (i.e., the formation of CXCR5$^+$PD-1^{int} pre-T_{FH} cells) but not sufficient for the differentiation of CXCR5$^+$PD-1^{hi} T_{FH} cells (29, 65), and B cells are required for the differentiation and maintenance of CXCR5$^+$PD-1^{hi} T_{FH} cells (66, 67). We used the CD11c-DTR mice, as an inducible depletion model for CD11c$^+$ cells, to study the impact of depleting CD11c$^+$ cells on established T_{FH} responses at day 10 in the Bm12 cGVHD model (68) (Fig. 7*C*). Diphtheria toxin (DT) treatment led to a significant reduction of CD11c$^+$ ABCs in CD11c-DTR mice (Fig. 7 *D* and *E*). Importantly, we also observed a significant reduction in CXCR5$^+$PD-1^{hi} T_{FH} levels (Fig. 7 *F* and *G*), as well as T_{EM} levels (Fig. 7 *H* and *I*), suggesting that CD11c$^+$ ABCs contribute to the maintenance of T_{FH} responses.

CD11c$^+$Tbet$^+$ ABCs Correlate with T_{FH} Cells in Lupus Patients. To further investigate whether CD11c$^+$Tbet$^+$ ABCs correlate with T_{FH} cells in lupus patients, we analyzed CD11c$^+$ ABCs in human systemic lupus erythematosus (SLE) patients (*SI Appendix*, Table S1). CD11c$^+$ ABCs were identified using previously described surface markers as CD19$^+$IgD$^-$CD21$^-$CD11c$^+$ cells (Fig. 8*A*) and confirmed to express Tbet (Fig. 8*B*). Significantly more CD11c$^+$ ABCs were observed in SLE patients as compared to healthy controls (Fig. 8 *A* and *C*), consistent with previous reports (35, 69). At the same time, we observed significantly increased CD4$^+$CXCR5$^+$ICOS$^+$PD-1^{hi} cells, a T_{FH} subset referred to as recently activated memory T_{FH} cells (70, 71), in SLE patients (Fig. 8 *D* and *E*). Notably, the levels of these cells and CD11c$^+$ ABCs correlate in SLE patients (Fig. 8*F*), suggesting that the cross-talk between CD11c$^+$ ABC and T_{FH} cells we observe in lupus mice may also operate in lupus patients.

Discussion

Our study shows that antigen-specific GC responses are compromised in all tested lupus models, with significantly reduced differentiation of antigen-specific GCB cells and impaired AAM, highlighting a humoral immunodeficiency that has not been sufficiently appreciated. Our data suggest that this defect is not due to the reduced formation of GC or GCB cells, but rather due to the lack of efficient affinity-based positive selection for antigen-specific GCB cells, the basis of the production of pathogen-specific affinity-matured antibodies.

Strikingly, our data support that this defect can be triggered by excessive CD11c$^+$Tbet$^+$ ABCs, a non-GCB cell subset. In Ship$^{\Delta B}$ mice, a B cell-intrinsic lupus model, excessive CD11c$^+$Tbet$^+$ ABCs emerge before deregulated T-cell activation and T_{FH} differentiation, as well as autoantibody production. Our study shows that excessive CD11c$^+$Tbet$^+$ ABC differentiation in Ship$^{\Delta B}$ mice promotes deregulated T-cell activation and T_{FH} differentiation through their potent antigen-presenting function and consequently compromises GCB-cell selection and AAM. Consistently, it has been shown that B cells are required for T_{FH} differentiation and maintenance (66, 67). Our observation that depleting CD11c$^+$ cells attenuates established T_{FH} responses in Bm12 cGVHD mice suggests that CD11c$^+$ ABCs contribute to T_{FH} maintenance. Notably, it has been reported that selectively depleting CD11c$^+$ B cells leads to ~80% reduction in T_{FH} cells (72), which was interpreted as the impact of depleting GCB cells based on the observation that a small fraction (~20%) of GC B cells express CD11c (72). In the context of our study, these data can be alternatively interpreted as the impact of depleting CD11c$^+$ ABCs, which constitute the majority of CD11c$^+$ B cells (50 to ~80%, as compared to ~10% for GC B cells).

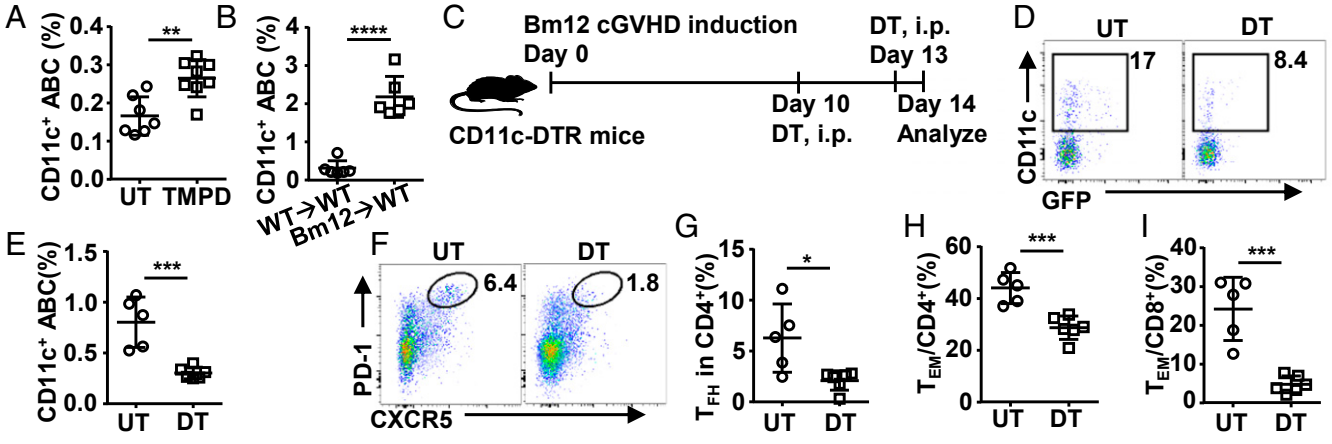

Fig. 7. The maintenance of T_{FH} responses requires CD11c$^+$ cells. (*A* and *B*) The percentage of CD11c$^+$ ABCs among B cells in the spleen of TMPD-induced (*A*) and Bm12 cGVHD mice (*B*). (*C–J*) CD11c$^+$ B-cell deletion model (*C*): CD11c-DTR mice were transferred with Bm12 splenocytes on day 0, injected i.p. without (UT) or with diphtheria toxin (DT) on day 10 and day 13 (80 ng per mouse per dose), and analyzed on day 14 for the abundance of splenic CD11c$^+$ ABCs (also GFP$^+$), T_{FH}, and T_{EM}. The following data are presented: representative FACS profile (*D*) and bar graph (*E*) showing the percentage of CD11c$^+$ ABCs; representative FACS profile (*F*) and bar graph (*G*) showing the percentage of T_{FH} cells; bar graphs showing the percentage of CD44$^+$CD62L$^-$ effector/memory cells (T_{EM}) among CD4$^+$ (*H*) and CD8$^+$ (*I*) T cells. Each symbol in the bar graphs represents an individual mouse. Bars represent means ± SD. *$P \le 0.05$; **$P \le 0.01$; ***$P \le 0.001$; ****$P \le 0.0001$ (unpaired 2-tailed *t* test [*A*, *B*, *E*, *G*, *I*, and *J*]). A representative of 2 (*B–J*) or 3 (*A*) independent experiments is shown.

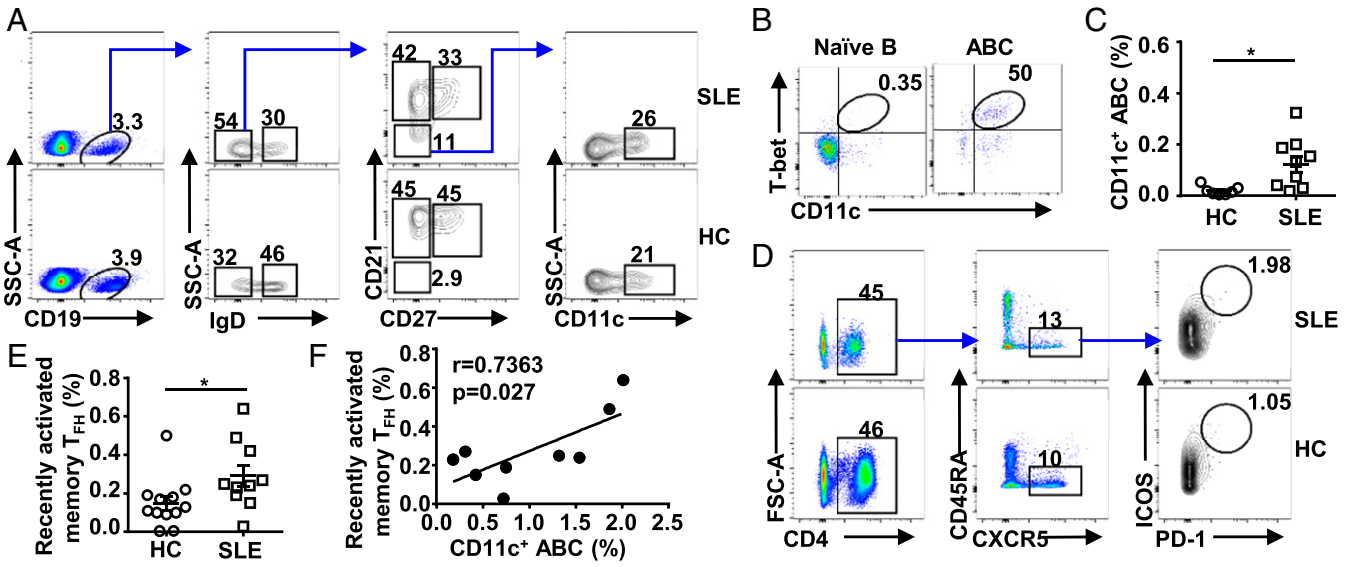

Fig. 8. $CD11c^+Tbet^+$ ABCs correlate with T_{FH} cells in lupus patients. (*A*) Gating strategy of $CD11c^+$ ABCs in peripheral blood of SLE patients and healthy donors. (*B*) Representative FACS profile showing Tbet expression in naïve B cells ($CD19^+IgD^+CD27^-CD21^+$) and ABCs ($CD19^+IgD^+CD27^-CD21^-$) in SLE patients. (*C*) The percentage of $CD11c^+$ ABCs among B cells in healthy donors and SLE patients. (*D*) Gating strategy of recently activated memory T_{FH} cells in peripheral blood of SLE patients and healthy donors. (*E*) The percentage of recently activated memory T_{FH} cells among $CD4^+$ T cells in healthy donors and SLE patients. (*F*) Correlation between the percentage of $CD11c^+$ ABCs among B cells and recently activated memory T_{FH} cell percentage among $CD4^+$ T cells in SLE patients. Each symbol in the bar graphs represents an individual mouse or human. Bars represent means ± SEM. $*P \leq 0.05$ (unpaired 2-tailed *t* test [*C* and *E*]; *r* and *P* values, linear regression [*F*]). A representative of 3 (*A*, *B*, and *D*) independent experiments is shown. *C*, *E*, and *F* are summarized from multiple experiments.

Our model is further supported by the observation that inhibiting $CD11c^+$ ABC differentiation in $Ship^{\Delta B}$ mice by ablating B cell-intrinsic MyD88 not only normalizes T_{FH} differentiation but also rescues GC selection and AAM. B cell-intrinsic MyD88 has also been reported to be critical for GCB-cell and antibody responses to TLR ligand-containing vaccines/immunizations (73, 74), as well as for Breg differentiation (75). However, it seems that neither GCB cells nor Breg cells are likely to mediate the rescue effect of ablating B cell-intrinsic MyD88 in $Ship^{\Delta B}$ mice as ablating MyD88 in GCB cells ($MyD88^{\Delta B}$ mice) does not significantly change NP-specific GC responses and ablating B cell-intrinsic MyD88 has been shown to inhibit Breg differentiation and exacerbate autoimmunity (75–77). Also consistent with our model, impaired AAM has also been reported in aged mice (78), where increased ABCs were originally described (32, 33). To the best of our knowledge, non-GCB cell-intrinsic mechanisms that regulate GCB-cell selection have barely been described, nor has their impact on T_{FH} differentiation.

A striking finding in our study is that excessive $CD11c^+Tbet^+$ ABCs not only compromise GCB-cell selection and AAM but also promote autoantibody production, which leads to the production of "poor" low-affinity antigen-specific antibodies and "bad" autoantibodies in lupus mice at the same time. It suggests that excessive autoantibodies and inadequate affinity-matured antigen-specific antibodies observed in these models—2 seemly paradoxical humoral immune defects—is mechanistically linked by excessive $CD11c^+Tbet^+$ ABCs. The impact of $CD11c^+Tbet^+$ ABCs on GC selection and AAM observed in our study is distinct from that on autoimmunity described previously (33–36, 38) and confirmed in this study. Nevertheless, it appears that their ability to promote T-cell activation and T_{FH} differentiation may explain these distinct impacts, as excessive T_{FH} cells have also been proposed to drive the development of spontaneous GCs associated with autoimmunity (23, 24).

While increased $CD11c^+Tbet^+$ ABCs have been described in aged and autoimmune murine models, as well as in autoimmune patients (34), the initial triggers for their differentiation are not fully understood. Their superior potency over FOB cells in priming T cells suggests that $CD11c^+Tbet^+$ ABCs are antigen-experienced cells. Consistently, $CD11c^+Tbet^+$ ABCs were shown to have selected BCR repertoire (79), with more somatic hypermutations than FOB cells but less than GCB cells (80). Our study also provided in vivo data supporting that $CD11c^+Tbet^+$ ABC differentiation depends on TLR signaling adaptor MyD88, consistent with the previous finding that IL-21 and TLR7 stimulation cooperate to drive Tbet expression (38, 39) and that $CD11c^+Tbet^+$ ABCs are highly responsive to TLR7 stimulation (34, 38).

Many studies of humoral immune responses in lupus focus on immune tolerance, rather than the quality of the antibodies that are meant to provide immunity. Given the compromised GC selection and AAM in lupus mice, and the increased $CD11c^+Tbet^+$ ABCs and correlated T_{FH} cells in lupus patients, we speculate that a similar GC selection and AAM defect also exists in lupus and lupus-like cGVHD patients. The contribution of $CD11c^+Tbet^+$ ABCs to "poor" low-affinity antibodies and "bad" autoantibodies in our murine models suggests that these cells and their dependent signalings (TLR signaling, e.g.) may be potential targets for treating these diseases. Further study will help us to better understand humoral immune responses in lupus and cGVHD patients (7–13), as well as to develop new therapies.

Materials and Methods

Human Subjects. Eleven SLE patients and 19 healthy controls were enrolled in this study. Patients fulfilled the American College of Rheumatology 1997 revised criteria for SLE. Healthy controls were recruited from the medical center matched to SLE patients with age and sex. Ethical approval was obtained from the Ethics Committee of Shanghai Changzheng Hospital. Informed consent was obtained from all study subjects. Clinical and demographic data were collected from their medical records. Additional clinical information about the subjects is listed in *SI Appendix*, Table S1.

Mouse Models. WT mice were injected with 500 μL of TMPD (P7820; Sigma-Aldrich) or 1×10^7 Bm12 splenocytes per mouse through intraperitoneal injection to induce TMPD or Bm12 cGVHD lupus models. Both TMPD-induced and Bm12 cGVHD mice were used after 2 wk of induction. For $CD11c^+$ cell deletion study, CD11c-DTR mice were transferred with Bm12 splenocytes on day 0 to induce Bm12 cGVHD models and intraperitoneally (i.p.) injected

with DT (322326; Sigma) on day 10 and day 13 at a dosage of 80 ng per mouse and analyzed on day14. All mice were maintained in the specific pathogen-free animal facility at Shanghai Jiao Tong University School of Medicine (SJTUSM). All animal experiments were performed in compliance with institutional guidelines and had been approved by the SJTUSM Institutional Animal Care and Use Committee.

NP-Specific Responses. Ten- to ∼12-wk-old mice immunized i.p. with NP_{45}-CGG (100 μg/mouse [N-5055E; Biosearch Technologies]) in alum (77161; Pierce) 2 wk earlier were analyzed by fluorescence-assisted cell sorting (FACS). V186.2-Cγ1 fragments were amplified from total splenic mRNA and subjected to next-generation sequencing and MiXCR analysis (81) for W33L mutation rates. For B1-8^{hi} cell transfer experiments, 5×10^6 B1-8^{hi} or $Ship^{\Delta B}$ -B1-8^{hi} splenocytes alone or mixed 1:1 with B1-8^{lo} splenocytes were transferred intravenously (i.v.). For T–B cell cotransfer, mice were transferred i.v. with 1×10^7 magnetic-activated cell-sorting-purified splenic pan-T and 2×10^6 B1-8^{hi} B cells (130-095-130 and 130-090-862; Miltenyi Biotec) and immunized with NP_{45}-CGG/alum the day after and analyzed 10 d after immunization.

Additional methods are listed in *SI Appendix, Methods*. This includes a detailed description of mice, FACS (flow cytometry), B-cell purification, $CD11c^+$ ABC differentiation and T-cell activation, autoantibodies, RNA sequencing, immunofluorescence, Western blot, in vitro test of antigen presentation, and statistical analysis.

ACKNOWLEDGMENTS. We thank Drs. Jeffrey Ravetch (The Rockefeller University) and Garnett Kelsoe (Duke University) for generously providing $Ship^{\Delta B}$ mice and NB-21.2D9 feeder cells, respectively, and Dr. Yuan Zhuang for helpful discussions. This work was supported by Chinese Mega Project on Infectious Diseases Grant 2018ZX10302301, National Natural Science Foundation of China (NNSFC) Project 31422020, 973 Program 2014CB943600, and NNSFC Projects 31600704 and 31800778. F.L. is supported by the "Shu Guang" project from Shanghai Municipal Education Commission and Shanghai Education Development Foundation. H.Z. is supported by the Program for Professor of Special Appointment (Eastern Scholar) at Shanghai Institutions of Higher Learning. H.Z., Y.Z., and F.L. are also supported by Innovative research team of high-level local universities in Shanghai.

1. R. Brink, T. G. Phan, Self-reactive B cells in the germinal center reaction. *Annu. Rev. Immunol.* **36**, 339–357 (2018).
2. D. L. Burnett *et al*., Germinal center antibody mutation trajectories are determined by rapid self/foreign discrimination. *Science* **360**, 223–226 (2018).
3. R. E. Schmidt, B. Grimbacher, T. Witte, Autoimmunity and primary immunodeficiency: Two sides of the same coin? *Nat. Rev. Rheumatol.* **14**, 7–18 (2017).
4. J. S. Weinstein *et al*., Colocalization of antigen-specific B and T cells within ectopic lymphoid tissue following immunization with exogenous antigen. *J. Immunol.* **181**, 3259–3267 (2008).
5. M. Kimura, E. Gleichmann, Depressed antibody responses to exogenous antigens in mice with lupus-like graft-versus-host disease. *Clin. Immunol. Immunopathol.* **43**, 97–109 (1987).
6. W. H. Leung *et al*., Aberrant antibody affinity selection in SHIP-deficient B cells. *Eur. J. Immunol.* **43**, 371–381 (2013).
7. A. Mathian, M. Pha, Z. Amoura, Lupus and vaccinations. *Curr. Opin. Rheumatol.* **30**, 465–470 (2018).
8. R. P. Rezende *et al*., Immunogenicity of pneumococcal polysaccharide vaccine in adult systemic lupus erythematosus patients undergoing immunosuppressive treatment. *Lupus* **25**, 1254–1259 (2016).
9. K. Sacre *et al*., Impaired long-term immune protection following pneumococcal 13-valent/23-valent polysaccharide vaccine in systemic lupus erythematosus (SLE). *Ann. Rheum. Dis.* **77**, 1540–1542 (2018).
10. A. Danza, G. Ruiz-Irastorza, Infection risk in systemic lupus erythematosus patients: Susceptibility factors and preventive strategies. *Lupus* **22**, 1286–1294 (2013).
11. F. E. Ospina *et al*., Distinguishing infections vs flares in patients with systemic lupus erythematosus. *Rheumatology (Oxford)* **56** (suppl. 1), i46–i54 (2017).
12. G. Socié, J. Ritz, Current issues in chronic graft-versus-host disease. *Blood* **124**, 374–384 (2014).
13. J. L. Ferrara, H. J. Deeg, Graft-versus-host disease. *N. Engl. J. Med.* **324**, 667–674 (1991).
14. G. D. Victora, M. C. Nussenzweig, Germinal centers. *Annu. Rev. Immunol.* **30**, 429–457 (2012).
15. L. Mesin, J. Ersching, G. D. Victora, Germinal center B cell dynamics. *Immunity* **45**, 471–482 (2016).
16. O. Bannard, J. G. Cyster, Germinal centers: Programmed for affinity maturation and antibody diversification. *Curr. Opin. Immunol.* **45**, 21–30 (2017).
17. H. X. Liao *et al*.; NISC Comparative Sequencing Program, Co-evolution of a broadly neutralizing HIV-1 antibody and founder virus. *Nature* **496**, 469–476 (2013).
18. L. Pappas *et al*., Rapid development of broadly influenza neutralizing antibodies through redundant mutations. *Nature* **516**, 418–422 (2014).
19. M. Muramatsu *et al*., Class switch recombination and hypermutation require activation-induced cytidine deaminase (AID), a potential RNA editing enzyme. *Cell* **102**, 553–563 (2000).
20. P. Revy *et al*., Activation-induced cytidine deaminase (AID) deficiency causes the autosomal recessive form of the Hyper-IgM syndrome (HIGM2). *Cell* **102**, 565–575 (2000).
21. Y. Takahashi, H. Ohta, T. Takemori, Fas is required for clonal selection in germinal centers and the subsequent establishment of the memory B cell repertoire. *Immunity* **14**, 181–192 (2001).
22. R. N. Pearse *et al*., SHIP recruitment attenuates Fc gamma RIIB-induced B cell apoptosis. *Immunity* **10**, 753–760 (1999).
23. A. Pratama, C. G. Vinuesa, Control of TFH cell numbers: Why and how? *Immunol. Cell Biol.* **92**, 40–48 (2014).
24. C. G. Vinuesa, M. A. Linterman, D. Yu, I. C. MacLennan, Follicular helper T cells. *Annu. Rev. Immunol.* **34**, 335–368 (2016).
25. M. A. Linterman *et al*., Follicular helper T cells are required for systemic autoimmunity. *J. Exp. Med.* **206**, 561–576 (2009).
26. J. Rolf *et al*., Phosphoinositide 3-kinase activity in T cells regulates the magnitude of the germinal center reaction. *J. Immunol.* **185**, 4042–4052 (2010).
27. C. Jacquemin *et al*., OX40 ligand contributes to human lupus pathogenesis by promoting T follicular helper response. *Immunity* **42**, 1159–1170 (2015).
28. P. T. Sage *et al*., Dendritic cell PD-L1 limits autoimmunity and follicular T cell differentiation and function. *J. Immunol.* **200**, 2592–2602 (2018).
29. L. G. Barnett *et al*., B cell antigen presentation in the initiation of follicular helper T cell and germinal center differentiation. *J. Immunol.* **192**, 3607–3617 (2014).
30. H. Xu *et al*., Follicular T-helper cell recruitment governed by bystander B cells and ICOS-driven motility. *Nature* **496**, 523–527 (2013).
31. D. Liu *et al*., T-B-cell entanglement and ICOSL-driven feed-forward regulation of germinal centre reaction. *Nature* **517**, 214–218 (2015).
32. Y. Hao, P. O'Neill, M. S. Naradikian, J. L. Scholz, M. P. Cancro, A B-cell subset uniquely responsive to innate stimuli accumulates in aged mice. *Blood* **118**, 1294–1304 (2011).
33. A. V. Rubtsov *et al*., Toll-like receptor 7 (TLR7)-driven accumulation of a novel $CD11c^+$ B-cell population is important for the development of autoimmunity. *Blood* **118**, 1305–1315 (2011).
34. M. S. Naradikian, Y. Hao, M. P. Cancro, Age-associated B cells: Key mediators of both protective and autoreactive humoral responses. *Immunol. Rev.* **269**, 118–129 (2016).
35. Y. Liu *et al*., T-bet^+CD11c^+ B cells are critical for antichromatin immunoglobulin G production in the development of lupus. *Arthritis Res. Ther.* **19**, 225 (2017).
36. K. Rubtsova *et al*., B cells expressing the transcription factor T-bet drive lupus-like autoimmunity. *J. Clin. Invest.* **127**, 1392–1404 (2017).
37. M. Manni *et al*., Regulation of age-associated B cells by IRF5 in systemic autoimmunity. *Nat. Immunol.* **19**, 407–419 (2018).
38. S. A. Jenks *et al*., Distinct effector B cells induced by unregulated Toll-like receptor 7 contribute to pathogenic responses in systemic lupus erythematosus. *Immunity* **49**, 725–739.e6 (2018).
39. M. S. Naradikian *et al*., Cutting edge: IL-4, IL-21, and IFN-γ interact to govern T-bet and CD11c expression in TLR-activated B cells. *J. Immunol.* **197**, 1023–1028 (2016).
40. K. Rubtsova, P. Marrack, A. V. Rubtsov, TLR7, IFNγ, and T-bet: Their roles in the development of ABCs in female-biased autoimmunity. *Cell. Immunol.* **294**, 80–83 (2015).
41. L. L. Teichmann, D. Schenten, R. Medzhitov, M. Kashgarian, M. J. Shlomchik, Signals via the adaptor MyD88 in B cells and DCs make distinct and synergistic contributions to immune activation and tissue damage in lupus. *Immunity* **38**, 528–540 (2013).
42. A. V. Rubtsov *et al*., CD11c-expressing B cells are located at the T cell/B cell border in spleen and are potent APCs. *J. Immunol.* **195**, 71–79 (2015).
43. M. Satoh, W. H. Reeves, Induction of lupus-associated autoantibodies in BALB/c mice by intraperitoneal injection of pristane. *J. Exp. Med.* **180**, 2341–2346 (1994).
44. M. Satoh, A. Kumar, Y. S. Kanwar, W. H. Reeves, Anti-nuclear antibody production and immune-complex glomerulonephritis in BALB/c mice treated with pristane. *Proc. Natl. Acad. Sci. U.S.A.* **92**, 10934–10938 (1995).
45. M. Satoh *et al*., Widespread susceptibility among inbred mouse strains to the induction of lupus autoantibodies by pristane. *Clin. Exp. Immunol.* **121**, 399–405 (2000).
46. A. G. Rolink, S. T. Pals, E. Gleichmann, Allosuppressor and allohelper T cells in acute and chronic graft-vs.-host disease. II. F1 recipients carrying mutations at H-2K and/or I-A. *J. Exp. Med.* **157**, 755–771 (1983).
47. S. C. Morris, P. L. Cohen, R. A. Eisenberg, Experimental induction of systemic lupus erythematosus by recognition of foreign Ia. *Clin. Immunol. Immunopathol.* **57**, 263–273 (1990).
48. M. J. Maxwell *et al*., Genetic segregation of inflammatory lung disease and autoimmune disease severity in SHIP-1-/- mice. *J. Immunol.* **186**, 7164–7175 (2011).
49. S. K. O'Neill *et al*., Monophosphorylation of CD79a and CD79b ITAM motifs initiates a SHIP-1 phosphatase-mediated inhibitory signaling cascade required for B cell anergy. *Immunity* **35**, 746–756 (2011).
50. Y. Chen *et al*., SHIP-1 deficiency in AID^+ B cells leads to the impaired function of B10 cells with spontaneous autoimmunity. *J. Immunol.* **199**, 3063–3073 (2017).
51. D. C. Nacionales *et al*., B cell proliferation, somatic hypermutation, class switch recombination, and autoantibody production in ectopic lymphoid tissue in murine lupus. *J. Immunol.* **182**, 4226–4236 (2009).
52. W. Guo *et al*., Somatic hypermutation as a generator of antinuclear antibodies in a murine model of systemic autoimmunity. *J. Exp. Med.* **207**, 2225–2237 (2010).
53. M. J. Shlomchik, A. Marshak-Rothstein, C. B. Wolfowicz, T. L. Rothstein, M. G. Weigert, The role of clonal selection and somatic mutation in autoimmunity. *Nature* **328**, 805–811 (1987).
54. T. A. Shih, M. Roederer, M. C. Nussenzweig, Role of antigen receptor affinity in T cell-independent antibody responses in vivo. *Nat. Immunol.* **3**, 399–406 (2002).

55. T. Inoue *et al*., The transcription factor Foxo1 controls germinal center B cell proliferation in response to T cell help. *J. Exp. Med.* **214**, 1181–1198 (2017).
56. K. Furukawa, A. Akasako-Furukawa, H. Shirai, H. Nakamura, T. Azuma, Junctional amino acids determine the maturation pathway of an antibody. *Immunity* **11**, 329–338 (1999).
57. S. Casola *et al*., Tracking germinal center B cells expressing germ-line immunoglobulin gamma1 transcripts by conditional gene targeting. *Proc. Natl. Acad. Sci. U.S.A.* **103**, 7396–7401 (2006).
58. A. D. Gitlin, Z. Shulman, M. C. Nussenzweig, Clonal selection in the germinal centre by regulated proliferation and hypermutation. *Nature* **509**, 637–640 (2014).
59. Z. Shulman *et al*., Dynamic signaling by T follicular helper cells during germinal center B cell selection. *Science* **345**, 1058–1062 (2014).
60. T. Hayashi *et al*., Prevention of autoimmune disease by induction of tolerance to Toll-like receptor 7. *Proc. Natl. Acad. Sci. U.S.A.* **106**, 2764–2769 (2009).
61. L. M. Sly, M. J. Rauh, J. Kalesnikoff, C. H. Song, G. Krystal, LPS-induced upregulation of SHIP is essential for endotoxin tolerance. *Immunity* **21**, 227–239 (2004).
62. H. An *et al*., Src homology 2 domain-containing inositol-5-phosphatase 1 (SHIP1) negatively regulates TLR4-mediated LPS response primarily through a phosphatase activity- and PI-3K-independent mechanism. *Blood* **105**, 4685–4692 (2005).
63. J. Tomic *et al*., Sensitization of IL-2 signaling through TLR-7 enhances B lymphoma cell immunogenicity. *J. Immunol.* **176**, 3830–3839 (2006).
64. B. Hou, B. Reizis, A. L. DeFranco, Toll-like receptors activate innate and adaptive immunity by using dendritic cell-intrinsic and -extrinsic mechanisms. *Immunity* **29**, 272–282 (2008).
65. R. Goenka *et al*., Cutting edge: Dendritic cell-restricted antigen presentation initiates the follicular helper T cell program but cannot complete ultimate effector differentiation. *J. Immunol.* **187**, 1091–1095 (2011).
66. H. Qi, T follicular helper cells in space-time. *Nat. Rev. Immunol.* **16**, 612–625 (2016).
67. Y. S. Choi *et al*., ICOS receptor instructs T follicular helper cell versus effector cell differentiation via induction of the transcriptional repressor Bcl6. *Immunity* **34**, 932–946 (2011).
68. J. Klarquist, E. M. Janssen, The bm12 inducible model of systemic lupus erythematosus (SLE) in C57BL/6 mice. *J. Vis. Exp.* **105**, e53319 (2015).
69. S. Wang *et al*.; Autoimmunity Molecular Medicine Team, IL-21 drives expansion and plasma cell differentiation of autoreactive CD11c^{hi}T-bet^{+} B cells in SLE. *Nat. Commun.* **9**, 1758 (2018).
70. M. Locci *et al*.; International AIDS Vaccine Initiative Protocol C Principal Investigators, Human circulating PD-1+CXCR3-CXCR5+ memory Tfh cells are highly functional and correlate with broadly neutralizing HIV antibody responses. *Immunity* **39**, 758–769 (2013).
71. J. He *et al*., Circulating precursor CCR7(lo)PD-1(hi) CXCR5^{+} CD4^{+} T cells indicate Tfh cell activity and promote antibody responses upon antigen reexposure. *Immunity* **39**, 770–781 (2013).
72. D. Baumjohann *et al*., Persistent antigen and germinal center B cells sustain T follicular helper cell responses and phenotype. *Immunity* **38**, 596–605 (2013).
73. B. Hou *et al*., Selective utilization of Toll-like receptor and MyD88 signaling in B cells for enhancement of the antiviral germinal center response. *Immunity* **34**, 375–384 (2011).
74. C. Pasare, R. Medzhitov, Control of B-cell responses by Toll-like receptors. *Nature* **438**, 364–368 (2005).
75. C. Mauri, A. Bosma, Immune regulatory function of B cells. *Annu. Rev. Immunol.* **30**, 221–241 (2012).
76. V. Lampropoulou *et al*., TLR-activated B cells suppress T cell-mediated autoimmunity. *J. Immunol.* **180**, 4763–4773 (2008).
77. P. Neves *et al*., Signaling via the MyD88 adaptor protein in B cells suppresses protective immunity during Salmonella typhimurium infection. *Immunity* **33**, 777–790 (2010).
78. R. Goenka, J. L. Scholz, M. S. Naradikian, M. P. Cancro, Memory B cells form in aged mice despite impaired affinity maturation and germinal center kinetics. *Exp. Gerontol.* **54**, 109–115 (2014).
79. A. Aranburu *et al*., Age-associated B cells expanded in autoimmune mice are memory cells sharing H-CDR3-selected repertoires. *Eur. J. Immunol.* **48**, 509–521 (2018).
80. L. M. Russell Knode *et al*., Age-associated B cells express a diverse repertoire of V_H and $V\kappa$ genes with somatic hypermutation. *J. Immunol.* **198**, 1921–1927 (2017).
81. D. A. Bolotin *et al*., MiXCR: Software for comprehensive adaptive immunity profiling. *Nat. Methods* **12**, 380–381 (2015).